Value of ^{68}Ga-labeled Bombesin Antagonist (RM2) in the Detection of Primary Prostate Cancer Comparing With [^{18}F]fluoromethylcholine PET/CT and mpMRI – a Phase I/II Study

Mohsen Beheshti (m.beheshti@salk.at)
County Hospital Salzburg University Hospital Salzburg: Landeskrankenhaus Salzburg - Universitatsklinikum der Paracelsus Medizinischen Privatuniversitat https://orcid.org/0000-0003-3918-3812

Pekka Taimen
University of Turku: Turun Yliopisto

Jukka Kemppainen
Turku PET Centre: Turun PET keskus

Ivan Jambor
University of Turku: Turun Yliopisto

Andre Müller
Life Molecular Imaging: Alliance Medical GmbH

Wolfgang Loidl
Ordensklinikum Linz Elisabethinen Hospital: Ordensklinikum Linz GmbH Elisabethinen

Esa Kähkönen
University of Turku: Turun Yliopisto

Meeri Käkelä
University of Turku: Turun Yliopisto

Mathias Berndt
Life Molecular Imaging: Alliance Medical GmbH

Andrew W. Stephens
Life Molecular Imaging: Alliance Medical GmbH

Heikki Minn
University of Turku: Turun Yliopisto

Werner Langsteger
Medical University of Vienna: Medizinische Universitat Wien

Research Article

Keywords: Prostate cancer, bombesin antagonist, [68Ga]Ga-RM2, [18F]FCH, PET/CT, mpMRI

Posted Date: September 17th, 2021

DOI: https://doi.org/10.21203/rs.3.rs-809326/v1

Abstract

Purpose: Overexperssion of Gastrin-releasing-peptide receptor (GRPr) in prostate carcinoma (PCa) suggests new means in the detection of prostate cancer foci. The bombesin derivative RM2 (DOTA-4-amino-1-carboxymethylpiperidine-D-Phe-Gln-Trp-Ala-Val-Gly-His-Sta-Leu-NH2) is a GRPr antagonist with strong binding affinity. Based on promising results from a first-in-man study on PCa detection in patients with local disease, a Phase I/II study was initiated and the ability of [^{68}Ga]Ga-RM2 PET/CT to detect PCa lesions was compared with [^{18}F]fluoromethylcholine ([^{18}F]FCH) PET/CT and multiparameteric prostate Magnetic Resonance Imaging (mpMRI).

Methods: This Phase I/II study was conductedwith a pre-specified interim analysis following the enrollment of 30 biopsy-positive PCa subjects, stratified into low, intermediate and high pretreatment risk of extra-glandular metastases with reference to NCCN criteria. Each subject had PCa detected by transrectal ultrasound guided prostate biopsy and subjects were scheduled to undergo prostatectomy with pelvic lymph node (LN) dissection in intermediate and high risk patients. Following administration of an intravenous dose of 140 MBq of [^{68}Ga]Ga-RM2,imaging was conducted at 60 min. p.i.. Twenty-five (25/30) subjects had concomitant [^{18}F]FCH PET/CT imaging. All patients underwent mpMRI. Intra-prostatic and pelvic nodal PET/CT findings were correlated with histopathologic results.

Results: High uptake of [^{68}Ga]Ga-RM2 was seen in pancreas and the urinary system with very low background uptake in the rest of the abdomen or thorax. Despite of high bladder activity, focal intraprostatic uptake was readily well detectable. Of overall 312 analyzed regions, 120 regions (4 to 8 lesions per-patient) showed abnormal finding in the prostate gland. In a region-based analysis overall sensitivity and specificity of [^{68}Ga]Ga-RM2 PET/CT in the detection of primary tumor were 74% and 90%, respectively; while it was 60% and 80% for [^{18}F]FCH PET/CT and 72% and 89% for mpMRI. Although, the overall sensitivity of [^{68}Ga]Ga-RM2 PET/CT was higher comparing to [^{18}F]FCH PET/CT and mpMRI; however, the statistical analysis showed only significant difference between [^{68}Ga]Ga-RM2 PET/CT and [^{18}F]FCH PET/CT in intermediate-risk group (P=0.01) and [^{68}Ga]Ga-RM2 PET/CT and mpMRT in high-risk group (p=0.03). [^{68}Ga]Ga-RM2 PET/CT correctly detected 2 histopathologically verified LN metastases in 2 high risk patients; while ^{18}F-FCH PET/CT only identified the LN lesion in 1 patient.

Conclusion: [^{68}Ga]Ga-RM2 is a promising new PET-tracer with a high detection rate for intraprostatic PCa. While index lesion detection rates were similar in both PET/CT studies, the improved specificity of [^{68}Ga]Ga-RM2 for canver versus BPH renders it notably better than [^{18}F]FCH in the detection of intraprostatic lesions. In addition, GRP-R-based imaging seems to play a complementary role to Choline-based imaging for full characterization of PCa extent, biopsy guidance in low and intermediate metastatic risk PCa patients and has the potential to discriminate them from whom of those at higher risks.

Trial Registeration number: EudraCT-Nr.: 2014-003027-21, Date: 10 June, 2014

Introduction

Given the multifocal nature of prostate cancer, the accurate imaging and determination of its extent remains among the most challenging malignancies. Prostate-specific antigen (PSA) and digital rectal examination following by transrectal ultrasound (TRUS) - guided biopsies are the standard approaches in primary assessment of prostate cancer [1]. Due to the low diagnostic accuracy of TRUS, systematic biopsies are frequently used for the detection of prostate cancer [1]. Nevertheless, approximately one-third of cancers are missed on initial systematic biopsies [2, 3] and the Gleason score is upgraded between biopsies and radical prostatectomy [4]. Additionally, attempts to improve prostate cancer detection by intensifying the biopsy technique have not proven successful and appear to cause an increase in the risk of complications [5]. Therefore, there is an increasing need for accurate imaging modalities to guide biopsy and avoid related complications.

Multiparametric Magnet Resonance Imaging (mpMRI) has been shown to improve diagnostic accuracy in the evaluation of intraglandular prostate cancer [6]. However, high inter-reader and inter-center variability has been reported limited wide-spread of mpMRI in men with diagnosed and/or suspected prostate cancer [6, 7].

Cancer diagnosis draws on the use of molecular imaging as one of its essential tools. Currently, positron emission tomography (PET)and computed tomography (CT) play a pivotal role among molecular imaging modalities, providing noninvasive information which is functional as well as anatomical. In the last decade, several PET radiotracers have been investigated through clinical trials to form an accurate depiction of intraglandular malignancies in the prostate [8–13]. PET/CT using ^{11}C- and ^{18}F-labeled choline has shown consistent reliability in diagnostic performance in the assessment of recurrent prostate cancer [9, 14]. However, its inability, in the preoperative setting, to accurately differentiate cancerous tissues from inflammatory lesions or benign prostatic hyperplasia (BPH) should be noted. [10].

Gastrin-releasing peptide receptor (GRPr) proteins are highly overexpressed in multiple human tumors and have been detected in 63–100% of human prostate cancer tissue [15, 16]. ^{68}Ga-labeled-DOTA-4-amino-1-carboxymethyl-piperidine-DPhe-Gln-Trp-Ala-Val-Gly-His-Sta-Leu-NH2 ([^{68}Ga]Ga-RM2) is a synthetic bombesin receptor antagonist with high binding affinity to GRPr [17]. [^{68}Ga]Ga-RM2 PET has shown significant potential for imaging of primary prostate cancer in previous preclinical studies [18, 19]. Recently, prospective clinical trials have been conducted using [^{68}Ga]Ga-RM2 PET/CT both in staging as well as recurrent prostate cancer. The primary results showed promising results [20, 21].

Because [^{68}Ga]Ga-RM2 and ^{18}F-Choline target different biologic processes, understanding how these two tracers behave in PCa patients with different tumor characteristics and risk of metastases is essential for determining the best management scenario.

In the present prospective two-center clinical trial, we conducted a comparison of the diagnostic potential of PET/CT imaging to detect primary prostate cancer with [^{68}Ga]Ga-RM2, as a novel PET tracer, and

imaging using [^{18}F]fluoromethyl-dimethyl-2-hydroxyethylammonium ([^{18}F]FCH) and correlated the results with mpMRI. In addition, we examined how diagnostic performance of these two tracers and mpMRI in low-, intermediate- and high-risk prostate cancer patients for intraprostatic cancer detection and extraglandular metastases. To our best knowledge, this is the earliest instance of such a study design being conducted with humans.

Materials And Methods

Patients

This prospective Phase I/II two-center clinical trial was performed in accordance with the principles of the 1964 Declaration of Helsinki and its later amendments or comparable standards and was approved by both the ethics committee of the Upperaustria and the Turku University Hospital. The study has been also registered in the European Clinical Trial Register with the register number of EudraCT-Nr.: 2014-003027-21. Signatures of the written informed consent were obtained from all subjects of the study.

The study was performed in primary staging of 30 men with biopsy proven prostate cancer. The patients were stratified into high- (10 patients), intermediate- (10 patients) and low-risk (10 patients) for extra-glandular metastases as defined by National Comprehensive Cancer Network (NCCN) criteria [22].

The inclusion and exclusion criteria are shown in supplement 1. Radical prostatectomy was performed in all patients within maximum interval of 4 weeks after completeing the imaging modalities. In 4 patients, an old partial transurethral prostatectomy has been performed which was not pointed out by patients and was not apparent in the primary medical history of these patients. Therefore, they were excluded to avoid any bias in the results of this study. The data from 26 patients (9 low-risk, 8 Intermediate-risk and 9 high-risk) were finally analyzed.

Safety monitoring included physical examination, electrocardiography, and laboratory parameters of various organs was performed during the [^{68}Ga]Ga-RM2 PET/CT examination and 24 hours as well as 3–5 days after radiotracer injection. Adverse events were documented.

PET-CT Imaging and Data Analysis

The patients underwent [^{68}Ga]Ga-RM2 PET/CT and [^{18}F]FCH PET/CT (all except 3 patients) with a maximum interval of 30 days (average: 8.7 days, range: 1–29 days). At least 2 weeks interval has been considered between prostate biopsy and imaging modalities. The study was performed with dedicated PET/CT scanners based on standard protocols (Supplement 2).

One experienced nuclear medicine specialist from each center, who only had knowledge of each patient's diagnosis interpreted all of the PET scans. Further, they were given access to the CT as well as PET-CT fusion images for morphological correlation and localization of pathological PET lesions. All discordant

findings have been evaluated in a multidisciplinary consensus meeting with related specialists of both centers for final interpretation.

Prostate gland was classified in 12 anatomic segments (apical, middle, and basal thirds, each divided into four segments of right, left, anterior, and posterior), for data analysis of both imaging as well as histopathologic findings.

A lesion was considered pathologic when the focal tracer accumulation was greater than the background activity. Semi-quantitative analysis of the abnormal radiotracer uptake was performed using the maximum standardized uptake value (SUVmax) within the volume of interest, manually placed over the pathological lesions on each anatomic section. The segment with the highest tracer intensity was defined as “index lesion” for the correlation with the segment with maximum tumor involvement on histopathology.

The final diagnosis of positive PET lesions was based on histopathological findings as “gold standard”, defined by a consensus interpretation of one experienced pathologist from each center.

MRI – Imaging and Data Analysis

Each patient was examined in a supine position in 1.5T (n = 23) and 3T (n = 3) scanners (Siemens, Erlangen, Germany) using surface phased-array coils or a combination of surface phased-array coils and endorectal coil. The MRI protocol at each institution consisted of T1W turbo spin echo (TSE) sequence in axial plane to exclude post-bioptic hemorrhage, T2W TSE sequences in axial (orthogonal to the urethra), coronal and sagittal planes. Diffuse weighted image (DWI) performed with echo-planar read-out obtained in transverse plane parallel to the transverse T2W to with apparent diffusion coefficient (ADC) maps reconstructed using the standard manufacture software. The 3D volume of the entire prostate was covered. Further details of prostate MRI protocol are presented in supplement 2.

MR data sets [T2-weighted (T2W), apparent diffusion coefficient (ADC), and dynamic contrast enhanced (DCE)] were evaluated in the daily work routine through consensus of two radiologists. The radiologists had knowledge of the confirmation of the tumour by way of autopsy; no information regarding the clinical stage and prostate specific antigen level was available. T2W and DWI images including ADC maps, and DCE results were interpreted qualitatively based on PI-RADS (version 2.1) scoring system for the tumor detection and localization.

Histopathological Analysis

Prostatectomy specimens were fixed in 10% buffered formalin for 24–48 hours and surgical margins were marked with different colors of tissue-ink to preserve the orientation and to allow for correlation with imaging datasets. Whole-mount prostatectomy macro-sections were obtained at 4–6-mm intervals transversely in a plane perpendicular to the long axis of the prostate gland in the superior–inferior direction. The most apical and basal macro-sections were further sectioned in coronal orientation to

evaluate any extraprostatic cancer extension at apex/basis or seminal vesicle invasion. Four μm sections from each paraffin block were cut, stained with hematoxylin–eosin and reviewed by two board-certified genitourinary pathologists. Gleason scores were assigned to all the lesions as combinations of primary, secondary, and tertiary Gleason grade, as defined by the 2014 International Society of Urological Pathology Modified Gleason Grading System[23]. If a Gleason grade pattern higher than the primary and secondary grade was present and visually accounted for less than 5% of the tumor volume, it was assigned as tertiary Gleason grade. Only PCa lesions with a diameter > 5 mm were considered clinically significant in the final correlation analyses with imaging findings.

Statistical Analysis

Univariate analysis was performed to assess the variables and frequency tables. Quantitative variables were defined as the mean ± SD and were compared in different groups using the independent t-test. The paired t-test was used to compare quantitative variables in a paired group. Sensitivity and specificity were calculated using data collected from PET studies on per-region base. Clopper-Pearson's correlation coefficient was calculated for correlations between different quantitative variables. Statistical analysis was conducted using SPSS software version 24 (SPSS Inc., Chicago, IL, USA). A value of $p < 0.05$ was considered to indicate statistical significance in all comparisons.

Results

Biodistribution and Safety

No adverse clinical reactions, abnormal laboratory findings, or side effects were detected during the 3–5 days after intravenous administration of [^{68}Ga]Ga-RM2.

High physiological [^{68}Ga]Ga-RM2 uptake was recorded in pancreas and, because of its renal excretion, in the urinary tract. Mild to moderate increased uptake was observed in the gastrointestinal tract. Liver, spleen. Bone marrow showed no noticeable physiological uptake (Fig. 1–4, A).

Primary tumor

[^{68}Ga]Ga-RM2 PET/CT was able to detect at least 1 index lesion in prostate gland in 83% (20/24) of patients with positive results in the final histopathology; while, [^{18}F]FCH PET/CT and mpMRI detected at least 1 index lesion in 76% (16/21) and 96% (23/24) of patients, respectively (Fig. 1).

In 2 low-risk patients with initially positive biopsy reports, final histopathology showed only 2 and 5 mm microfoci of Gleason 3 + 3 carcinoma but no of clinically significant for the final correlation analyses with imaging findings.

Region – based analysis

Of overall 312 analyzed regions, 120 regions (4 to 8 lesions per-patient) showed abnormal finding in the prostate gland either on imaging modalities and/or on histopathology. Histopathological findings confirmed cancerous tissue in 50 (42%) regions, while 70 regions showed no evidence of tumor infiltration (Table 1). Overall sensitivity and specificity of [^{68}Ga]Ga-RM2 PET/CT, [^{18}F]FCH PET/CT and mpMRI in the detection of primary tumor were 74% [95% confidence interval (95% CI) 62–86] and 90% (95% CI 83–97), 60% (95% CI 46–74) and 80% (95% CI 70–90), and 72% (95% CI 60–84) and 89% (95% CI 81–96), respectively. The sensitivity and specificity of each imaging modality in low-, intermediate-, and high-risk patients are presented in Table 2. Although, the overall sensitivity of [^{68}Ga]Ga-RM2 PET/CT was higher comparing to [^{18}F]FCH PET/CT and mpMRI; however, the statistical analysis showed only significant difference between [^{68}Ga]Ga-RM2 PET/CT and [^{18}F]FCH PET/CT in intermediate-risk group (P = 0.01) and [^{68}Ga]Ga-RM2 PET/CT and mpMRT in high-risk group (p = 0.03).

Table 1
Details of positive and negative histopathological findings in the region-based analysis.

Region	Number	Positive	Negative
overall	**120**	**50 (42%)**	**70 (58%)**
Low risk	36	13 (36%)	23 (64%)
Intermediate risk	40	20 (50%)	20 (50%)
High risk	44	17 (39%)	27 (61%)

Table 2

Region-based analysis: sensitivity and specificity of each imaging modality in low-, intermediate-, and high-risk patients

Sensitivity	[^{68}Ga]Ga-RM2	[^{18}F]FCH	mpMRI
overall	**74%**	**60%**	**72%**
Low risk	77%	69%	69%
Intermediate risk	80%	42%	55%
High risk	65%	73%	94%

Specificity	[^{68}Ga]Ga-RM2	[^{18}F]FCH	mpMRI
overall	**90%**	**80%**	**89%**
Low risk	83%	61%	87%
Intermediate risk	90%	94%	85%
High risk	96%	90%	93%

Lesion – based analysis

Overall, 56 lesions were analyzed in prostate gland on [^{68}Ga]Ga-RM2 PET/CT and mpMRI and 51 lesions on [^{18}F]FCH PET/CT. The difference between analyzed lesions was due to lack of performance of [^{18}F]FCH PET/CT in 3 patients. Histopathological results showed prostate cancer in 39 lesions. The sensitivity of [^{68}Ga]Ga-RM2 PET/CT, [^{18}F]FCH PET/CT and mpMRI in the detection of primary tumor was 74% (95% CI 61–88), 61% (95% CI 45–77), 67% (95% CI 52–82), respectively. The sensitivity as well as positive predictive value of each imaging modality in low-, intermediate-, and high-risk patients are displayed in Table 3.

Table 3
Lesion-based analysis: sensitivity, mean of maximum standardized uptake value (mean SUVmax) and positive predictive value (PPV) of each imaging modality in low-, intermediate-, and high-risk patients

Sensitivity	[^{68}Ga]Ga-RM2 (mean SUVmax, p-value)		[^{18}F]FCH (mean SUVmax)		mpMRI
overall	**74%**	**(5.98 ± 4.13; p=0-13)**	**61%**	**(6.08 ± 2.74)**	**67%**
Low risk	77%	(6.78±5.07; p=0.68)	62%	(6.05±2.11)	62%
Intermediate risk	80%	(6.16±3.67; P=0.13)	50%	(5.16±1.63)	53%
High risk	64%	(4.66±2.60; P=0.19)	78%	(6.45±3.30)	91%

PPV	[^{68}Ga]Ga-RM2	[^{18}F]FCH	mpMRI
overall	**81%**	**67%**	**79%**
Low risk	71%	50%	80%
Intermediate risk	80%	50%	53%
High risk	64%	78%	91%

There was no significant difference between SUVmax of [^{68}Ga]Ga-RM2 and [^{18}F]FCH PET/CT in the intra-prostatic malignant lesions ([^{68}Ga]Ga-RM2: mean SUVmax 5.98 ± 4.13; median: 4.75, [^{18}F]FCH: mean SUVmax 6.08 ± 2.74; median: 5.5; p = 0.13). A differentiation between malignant and BPH was not possible using a SUV-cutoff neither on [^{68}Ga]Ga-RM2 nor [^{18}F]FCH PET/CT. However, tumor to background ratio was 2.5 on ^{68}Ga-RM2 PET/CT comparing to 2.0 on [^{18}F]FCH PET/CT (p = 0.21). Although the mean SUVmax was higher in the low-risk and intermediate-risk comparing to high-risk patients on [^{68}Ga]Ga-RM2 PET/CT; however, the difference was not statistically significant and we didn't find any SUV-cutoff in order to predict the risk classification (Table 3). Also, there was no significant difference between mean SUVmax of various risk groups on [^{18}F]FCH PET/CT (Table 3).

Lymph node and distant metastases

Lymph node metastases were detected in 2 patients. In 1 high-risk patient with a PSA value of 30 ng/ml and Gleason score of 8 (4 + 4) with 4 regional lymph node metastases, [^{18}F]FCH PET/CT was able to detect 1 additional lymph node (diameter 15 mm) in the internal iliac region, which was negative on [^{68}Ga]Ga-RM2 PET/CT. Overall, the detected lymph nodes on [^{18}F]FCH PET/CT showed markedly higher uptake (mean SUVmax: 13.5 ± 3.72) comparing to [^{68}Ga]Ga-RM2 PET/CT (mean SUVmax: 3,92 ± 0.70), Fig. 2. In contrast, in another high-risk patient with PSA value of 4.9 ng/ml and Gleason score of 9 (4 + 5), [^{68}Ga]Ga-RM2 PET/CT detected 1 metastatic regional lymph node with a diameter of 9 mm in the external iliac region (SUVmax: 6.9), which was negative on [^{18}F]FCH PET/CT. No distant metastases were detected in our patient's population (Fig. 3).

Discussion

Data available concerning positron-emitting tracers which can reliably detect early prostate cancer and identify the extent of intraprostatic disease are limited. Thus, there is a tremendous need for an ideal tracer that can accurately detect the extent of intraprostatic cancer and differentiate malignant from BPH and inflammatory lesions.

The aim of the present study was to investigate the diagnostic accuracy of [^{68}Ga]Ga-RM2 PET/CT comparing to ^{18}F-FCH PET/CT and mpMRI in detection of primary prostate cancer. Furthermore, the pattern of tracer uptake on PET/CT was correlated with tumor characteristics on histopathology in low-, intermediate- and high-risk PCa patients.

In a region-based analysis the sensitivity and specificity of [^{68}Ga]Ga-RM2 PET/CT was superior to that of ^{18}F-FCH PET/CT and comparable to that of mpMRI. In overall assessment, there was no significant difference in diagnostic accuracy of different modalities. However, [^{68}Ga]Ga-RM2 PET/CT showed significantly higher sensitivity comparing [^{18}F]FCH PET/CT in intermediate-risk prostate cancer patients and mpMRI revealed significantly higher sensitivity in high-risk cases. In the lesion-based analysis,

overall, 39 PCa lesions were defined in histopathology. [^{68}Ga]Ga-RM2 PET/CT showed superior sensitivity of 74% in the detection of primary tumor comparing to [^{18}F]FCH PET/CT and mpMRI with a sensitivity of 61% and 67%, respectively. The overall findings of the present investigation are in concordance with similar studies [10, 18, 20, 24, 25]. To our best knowledge, this is the first prospective clinical investigation that explicitly evaluate the impact of [^{68}Ga]Ga-RM2 PET/CT and compare its value with [^{18}F]FCH PET/CT in three patients' cohorts with different metastatic risk stratifications, in which all patients underwent radical prostatectomy. When correlating the diagnostic accuracy of [^{68}Ga]Ga-RM2 PET/CT with biological tumor characteristics and metastatic risks, we noticed, both on region- and lesion-based analyses, limited sensitivity of 65% in high-risk patient's group comparing to 74% for [^{18}F]FCH PET/CT and 94% for mpMRI (Fig. 4). In contrast the [^{68}Ga]Ga-RM2 PET/CT showed significantly higher sensitivity of 80% in intermediate-risk cases comparing to 42% and 55% for [^{18}F]FCH PET/CT and mpMRI, respectively. These findings are not in line with the data presented by Kähkönen et. al., who reported markedly higher sensitivity of [^{68}Ga]Ga-RM2 PET/CT of 88% for the detection of primary tumor in 11 high-risk PCa patients [18]. This different sensitivity might be explained by the more advanced tumor stage in that study, as higher T-categories were reported in their patients comparing to our high-risk cohort [24]. Nevertheless, an accurate conclusion can not be drawn because of the low number of the patients in both studies.

In the last years, tremendous investigations have been done for developing radioligands targeting Prostate-specific-membrane-antigen (PSMA) for depiction of malignant tissues particularly in prostate cancer and several small-molecule tracers targeting PSMA have generated a lot of interest [26–28]. Although, numerous compounds labeled with different isotopes, leading probably by [^{68}Ga]Ga-HBED-PSMA [29] followed by [^{18}F]DCFPyl, have been tested in humans; however, none have been approved yet.

[^{68}Ga]Ga-PSMA and [^{18}F]PSMA tracers in conjunction with both PET/CT and PET/MRI have emerged as promising imaging modalities for primary staging and restaging of PCa [30–33]. However, there are still limited prospective data with large patient's population studied the impact of ^{68}Ga-labeled PSMA PET/CT for intraglandular detection of PCa. A subanalysis of prospective data of [^{68}Ga]Ga-PSMA PET/MRI in PCa showed significant differences in tracer uptake of the dominant intraprostatic cancer tissue between postoperative low/intermediate-risk patients and high-risk subjects [33]. In a recent preclinical study, the authors retrospectively compared the binding of radiolabeled GRPr-antagonists (i.e. [^{111}In]RM2) with [^{111}In]PSMA-617 in 20 frozen prostatectomy samples with various metastatic risks of the D'Amico classification [34]. They reported a significantly higher binding affinity of [^{111}In]RM2 in low metastatic risk samples with low Gleason score and low PSA value, while the binding of [^{111}In]PSMA-617 was high in almost all cancerous tissues independent to metastatic risk, Gleason score, or PSA value. The authors concluded that GRPr and PSMA-based imaging may have a complimentary role to fully characterize prostate cancer disease, GRPr being targeted in low metastatic risk patients while PSMA could be a valuable target in higher risks.

The findings of the current study support the data from previous investigations showing that [^{68}Ga]Ga-RM2 PET/CT detected more intraglandular prostate cancer lesions in low-risk group. However, we found no correlation between tracer uptake by means of SUVmax on [^{68}Ga]Ga-RM2 and [^{18}F]FCH PET/CT and Gleason score, PSA value and risk of metastases, in line with previous clinical reports [20, 24]. There was also no relevant trend in increasing pattern of SUVmax relating to PSA value and/or Gleason score. Although, the results of latter preclinical investigation agree with the known increased GRPr expression in low-grade prostate cancer; however, in-vitro and preclinical results may not necessarily represent the imaging findings on human.

In one of the early studies evaluating the impact of ^{68}Ga-labeled Bombesin antagonists in prostate cancer, the authors observed a significant difference in SUV between cancerous and hyperplastic prostatic lesions [18]. Although, less false positive intraprostatic lesions were seen on [^{68}Ga]Ga-RM2 PET comparing to [^{18}F]FCH PET (i.e. 7 versus 11, respectively), however, a differentiation between malignant and BPH was not possible using a SUV-cutoff neither by [^{68}Ga]Ga-RM2 nor [^{18}F]FCH PET/CT. The different findings may be related to the selection bias, as most of the patients undergoing a surgery in that study belonged to the high clinical risk group with high risk of lymph node metastasis.

Touijer et al. recently published clinical data in 16 patients with biopsy proven primary PCa with low (n = 2), intermediate (n = 8) and high risk (n = 6) of recurrence. The sensitivity, specificity and accuracy of 85.2%, 81.3% and 83.9% was reported for fused [^{68}Ga]Ga-RM2 PET/CT-mpMRI. The average SUVmax ranged from 1.5–27.8 with (mean: 9.1) for dominant tumors and 0.45–7.1 (mean:3.7) for BPH. However, no correlation was found between SUVmax with gleason score [20]. The higher diagnostic performance can be explained by using both [^{68}Ga]Ga-RM2 PET/CT and mpMRI findings and the higher number of patients with intermediate risk.

Despite the intention to gain information on extraprostatic metastases in the high risk group, only two case out of the 10 showed metastases, so limited conclusions can be made. In the detection of lymph node metastases, [^{68}Ga]Ga-RM2 and [^{18}F]FCH PET/CT showed contradicting findings in two high-risk PCa patients (Figs. 2 and 3). This may be related to PSA value in these patients, however, because of limited number of patients with lymph node metastases the impact of [^{68}Ga]Ga-RM2 PET/CT in the assessment of lymph node metastases remains inconclusive.

Our findings in this study may have future clinical impact. Prostate cancer patients with low metastatic risk are today not eligible for radical treatments anymore but rather to active surveillance or local treatments [35]. In addition, Gleason score is upgraded in about 30% of PCa patients between biopsies and radical prostatectomy [36]. Thus, an imaging procedure capable to discriminate “true” low and intermediate from high metastatic risks would be helpful to schedule local treatments in this group of patients. Results of this work indicate that GRPr targeting by hybrid imaging (e.g. PET/MRI) seems promising procedure amenable to better biopsy guidance in low and intermediate metastatic risk PCa patients and has the potential to discriminate them from PCa patients with higher risks. In addition, GRPr-

based imaging seems to play a complementary role to PSMA-based or Choline-based imaging for fully characterization of prostate cancer disease.

Conclusion

[^{68}Ga]Ga-RM2 is a promising new PET-tracer with a high detection rate for intraprostatic PCa. In addition, GRPr-based imaging seems to play a complementary role to Choline-based or PSMA-based imaging for fully characterization of prostate cancer disease, biopsy guidance in low and intermediate metastatic risk PCa patients and has the potential to discriminate them from whom of higher risks.

Declarations

Aknowledgment

The abstract of the results of this study has been presented in the “Clinical Oncology: Prostate” session(OP348) of the annual congress of European Society of Nuclear Medicine 2016 (EANM’16) in.

Funding

This study was funded by Life Molecular Imaging GmbH (previous Piramal Imaging GmbH), Berlin, Germany.

Conflicts of Interest

Andre Müller, Mathias Berndt, Andrew W. Stephens are employees of Life Molecular Imaging GmbH (previous Piramal Imaging GmbH), Berlin, Germany.

Other authors have no relevant financial or non-financial interests to disclose.

Ethics approval

This trial was performed in accordance with the principles of the 1964 Declaration of Helsinki and its later amendments or comparable standards and was approved by both the ethics committee of the Upperaustria and the Turku University Hospital. The study has been also registered in the European Clinical Trial Register with the register number of EudraCT-Nr.: 2014-003027-21.

Consent to participate

Signature of the written informed consent was obtained from all individual participants included in the study.

References

1. Halpern EJ, Frauscher F, Strup SE, Nazarian LN, O'Kane P, Gomella LG. Prostate: high-frequency Doppler US imaging for cancer detection. Radiology. 2002;225:71-7. doi:10.1148/radiol.2251011938.
2. Djavan B, Ravery V, Zlotta A, Dobronski P, Dobrovits M, Fakhari M, et al. Prospective evaluation of prostate cancer detected on biopsies 1, 2, 3 and 4: when should we stop? J Urol. 2001;166:1679-83.
3. Roehl KA, Antenor JA, Catalona WJ. Serial biopsy results in prostate cancer screening study. J Urol. 2002;167:2435-9.
4. Rajinikanth A, Manoharan M, Soloway CT, Civantos FJ, Soloway MS. Trends in Gleason score: concordance between biopsy and prostatectomy over 15 years. Urology. 2008;72:177-82. doi:10.1016/j.urology.2007.10.022.
5. Simon J, Kuefer R, Bartsch G, Jr., Volkmer BG, Hautmann RE, Gottfried HW. Intensifying the saturation biopsy technique for detecting prostate cancer after previous negative biopsies: a step in the wrong direction. BJU Int. 2008;102:459-62. doi:10.1111/j.1464-410X.2008.07560.x.
6. Hoeks CM, Barentsz JO, Hambrock T, Yakar D, Somford DM, Heijmink SW, et al. Prostate cancer: multiparametric MR imaging for detection, localization, and staging. Radiology. 2011;261:46-66. doi:10.1148/radiol.11091822.
7. Hricak H, Choyke PL, Eberhardt SC, Leibel SA, Scardino PT. Imaging prostate cancer: a multidisciplinary perspective. Radiology. 2007;243:28-53. doi:10.1148/radiol.2431030580.
8. Jadvar H. Molecular imaging of prostate cancer with 18F-fluorodeoxyglucose PET. Nat Rev Urol. 2009;6:317-23. doi:nrurol.2009.81 [pii] 10.1038/nrurol.2009.81.
9. Beheshti M, Haim S, Zakavi R, Steinmair M, Waldenberger P, Kunit T, et al. Impact of 18F-choline PET/CT in prostate cancer patients with biochemical recurrence: influence of androgen deprivation therapy and correlation with PSA kinetics. J Nucl Med.54:833-40. doi:jnumed.112.110148 [pii] 10.2967/jnumed.112.110148.
10. Vali R, Loidl W, Pirich C, Langesteger W, Beheshti M. Imaging of prostate cancer with PET/CT using (18)F-Fluorocholine. Am J Nucl Med Mol Imaging. 2015;5:96-108.
11. Dehdashti F, Picus J, Michalski JM, Dence CS, Siegel BA, Katzenellenbogen JA, et al. Positron tomographic assessment of androgen receptors in prostatic carcinoma. Eur J Nucl Med Mol Imaging. 2005;32:344-50. doi:10.1007/s00259-005-1764-5.
12. Kato T, Tsukamoto E, Kuge Y, Takei T, Shiga T, Shinohara N, et al. Accumulation of [11C]acetate in normal prostate and benign prostatic hyperplasia: comparison with prostate cancer. Eur J Nucl Med Mol Imaging. 2002;29:1492-5. doi:10.1007/s00259-002-0885-3.
13. Schuster DM, Savir-Baruch B, Nieh PT, Master VA, Halkar RK, Rossi PJ, et al. Detection of recurrent prostate carcinoma with anti-1-amino-3-18F-fluorocyclobutane-1-carboxylic acid PET/CT and 111In-capromab pendetide SPECT/CT. Radiology.259:852-61. doi:radiol.11102023 [pii] 10.1148/radiol.11102023.
14. Beheshti M, Langsteger W, Fogelman I. Prostate cancer: role of SPECT and PET in imaging bone metastases. Semin Nucl Med. 2009;39:396-407. doi:S0001-2998(09)00042-7 [pii] 10.1053/j.semnuclmed.2009.05.003.

15. Reubi JC, Wenger S, Schmuckli-Maurer J, Schaer JC, Gugger M. Bombesin receptor subtypes in human cancers: detection with the universal radioligand (125)I-[D-TYR(6), beta-ALA(11), PHE(13), NLE(14)] bombesin(6-14). Clin Cancer Res. 2002;8:1139-46.
16. Sun B, Halmos G, Schally AV, Wang X, Martinez M. Presence of receptors for bombesin/gastrin-releasing peptide and mRNA for three receptor subtypes in human prostate cancers. Prostate. 2000;42:295-303.
17. Jensen RT, Battey JF, Spindel ER, Benya RV. International Union of Pharmacology. LXVIII. Mammalian bombesin receptors: nomenclature, distribution, pharmacology, signaling, and functions in normal and disease states. Pharmacol Rev. 2008;60:1-42. doi:10.1124/pr.107.07108.
18. Kahkonen E, Jambor I, Kemppainen J, Lehtio K, Gronroos TJ, Kuisma A, et al. In vivo imaging of prostate cancer using [68Ga]-labeled bombesin analog BAY86-7548. Clin Cancer Res. 2013;19:5434-43. doi:10.1158/1078-0432.CCR-12-3490.
19. Zhang H, Desai P, Koike Y, Houghton J, Carlin S, Tandon N, et al. Dual-Modality Imaging of Prostate Cancer with a Fluorescent and Radiogallium-Labeled Gastrin-Releasing Peptide Receptor Antagonist. J Nucl Med. 2017;58:29-35. doi:10.2967/jnumed.116.176099.
20. Touijer KA, Michaud L, Alvarez HAV, Gopalan A, Kossatz S, Gonen M, et al. Prospective Study of the Radiolabeled GRPR Antagonist BAY86-7548 for Positron Emission Tomography/Computed Tomography Imaging of Newly Diagnosed Prostate Cancer. Eur Urol Oncol. 2019;2:166-73. doi:10.1016/j.euo.2018.08.011.
21. Minamimoto R, Sonni I, Hancock S, Vasanawala S, Loening A, Gambhir SS, et al. Prospective Evaluation of (68)Ga-RM2 PET/MRI in Patients with Biochemical Recurrence of Prostate Cancer and Negative Findings on Conventional Imaging. J Nucl Med. 2018;59:803-8. doi:10.2967/jnumed.117.197624.
22. NCCN Clinical Practice Guidelines in Oncology. Prostate Cancer
23. Epstein JI, Egevad L, Amin MB, Delahunt B, Srigley JR, Humphrey PA, et al. The 2014 International Society of Urological Pathology (ISUP) Consensus Conference on Gleason Grading of Prostatic Carcinoma: Definition of Grading Patterns and Proposal for a New Grading System. Am J Surg Pathol. 2016;40:244-52. doi:10.1097/PAS.0000000000000530.
24. Fassbender TF, Schiller F, Mix M, Maecke HR, Kiefer S, Drendel V, et al. Accuracy of [(68)Ga]Ga-RM2-PET/CT for diagnosis of primary prostate cancer compared to histopathology. Nucl Med Biol. 2019;70:32-8. doi:10.1016/j.nucmedbio.2019.01.009.
25. Husarik DB, Miralbell R, Dubs M, John H, Giger OT, Gelet A, et al. Evaluation of [(18)F]-choline PET/CT for staging and restaging of prostate cancer. Eur J Nucl Med Mol Imaging. 2008;35:253-63. doi:10.1007/s00259-007-0552-9.
26. Perera M, Papa N, Christidis D, Wetherell D, Hofman MS, Murphy DG, et al. Sensitivity, Specificity, and Predictors of Positive (68)Ga-Prostate-specific Membrane Antigen Positron Emission Tomography in Advanced Prostate Cancer: A Systematic Review and Meta-analysis. Eur Urol. 2016;70:926-37.

27. Cuccurullo V, Di Stasio GD, Mansi L. Nuclear medicine in prostate cancer: a new era for radiotracers. World J Nucl Med. 2018;17:70-8.
28. Lutje S, Heskamp S, Cornelissen AS, Poeppel TD, van den Broek SA, Rosenbaum-Krumme S, et al. PSMA Ligands for Radionuclide Imaging and Therapy of Prostate Cancer: Clinical Status. Theranostics. 2015;5:1388-401. doi:10.7150/thno.13348.
29. Afshar-Oromieh A, Malcher A, Eder M, Eisenhut M, Linhart HG, Hadaschik BA, et al. PET imaging with a [68Ga]gallium-labelled PSMA ligand for the diagnosis of prostate cancer: biodistribution in humans and first evaluation of tumour lesions. Eur J Nucl Med Mol Imaging. 2013;40:486-95. doi:10.1007/s00259-012-2298-2.
30. Budaus L, Leyh-Bannurah SR, Salomon G, Michl U, Heinzer H, Huland H, et al. Initial Experience of (68)Ga-PSMA PET/CT Imaging in High-risk Prostate Cancer Patients Prior to Radical Prostatectomy. Eur Urol. 2016;69:393-6. doi:10.1016/j.eururo.2015.06.010.
31. Eiber M, Weirich G, Holzapfel K, Souvatzoglou M, Haller B, Rauscher I, et al. Simultaneous (68)Ga-PSMA HBED-CC PET/MRI Improves the Localization of Primary Prostate Cancer. Eur Urol. 2016;70:829-36. doi:10.1016/j.eururo.2015.12.053.
32. Fendler WP, Schmidt DF, Wenter V, Thierfelder KM, Zach C, Stief C, et al. 68Ga-PSMA PET/CT Detects the Location and Extent of Primary Prostate Cancer. J Nucl Med. 2016;57:1720-5. doi:10.2967/jnumed.116.172627.
33. Grubmuller B, Baltzer P, Hartenbach S, D'Andrea D, Helbich TH, Haug AR, et al. PSMA Ligand PET/MRI for Primary Prostate Cancer: Staging Performance and Clinical Impact. Clin Cancer Res. 2018;24:6300-7. doi:10.1158/1078-0432.CCR-18-0768.
34. Schollhammer R, De Clermont Gallerande H, Yacoub M, Quintyn Ranty ML, Barthe N, Vimont D, et al. Comparison of the radiolabeled PSMA-inhibitor (111)In-PSMA-617 and the radiolabeled GRP-R antagonist (111)In-RM2 in primary prostate cancer samples. EJNMMI Res. 2019;9:52. doi:10.1186/s13550-019-0517-6.
35. Moschini M, Carroll PR, Eggener SE, Epstein JI, Graefen M, Montironi R, et al. Low-risk Prostate Cancer: Identification, Management, and Outcomes. Eur Urol. 2017;72:238-49. doi:10.1016/j.eururo.2017.03.009.
36. Porcaro AB, Siracusano S, de Luyk N, Corsi P, Sebben M, Tafuri A, et al. Low-Risk Prostate Cancer and Tumor Upgrading in the Surgical Specimen: Analysis of Clinical Factors Predicting Tumor Upgrading in a Contemporary Series of Patients Who were Evaluated According to the Modified Gleason Score Grading System. Curr Urol. 2017;10:118-25. doi:10.1159/000447164.

Figures

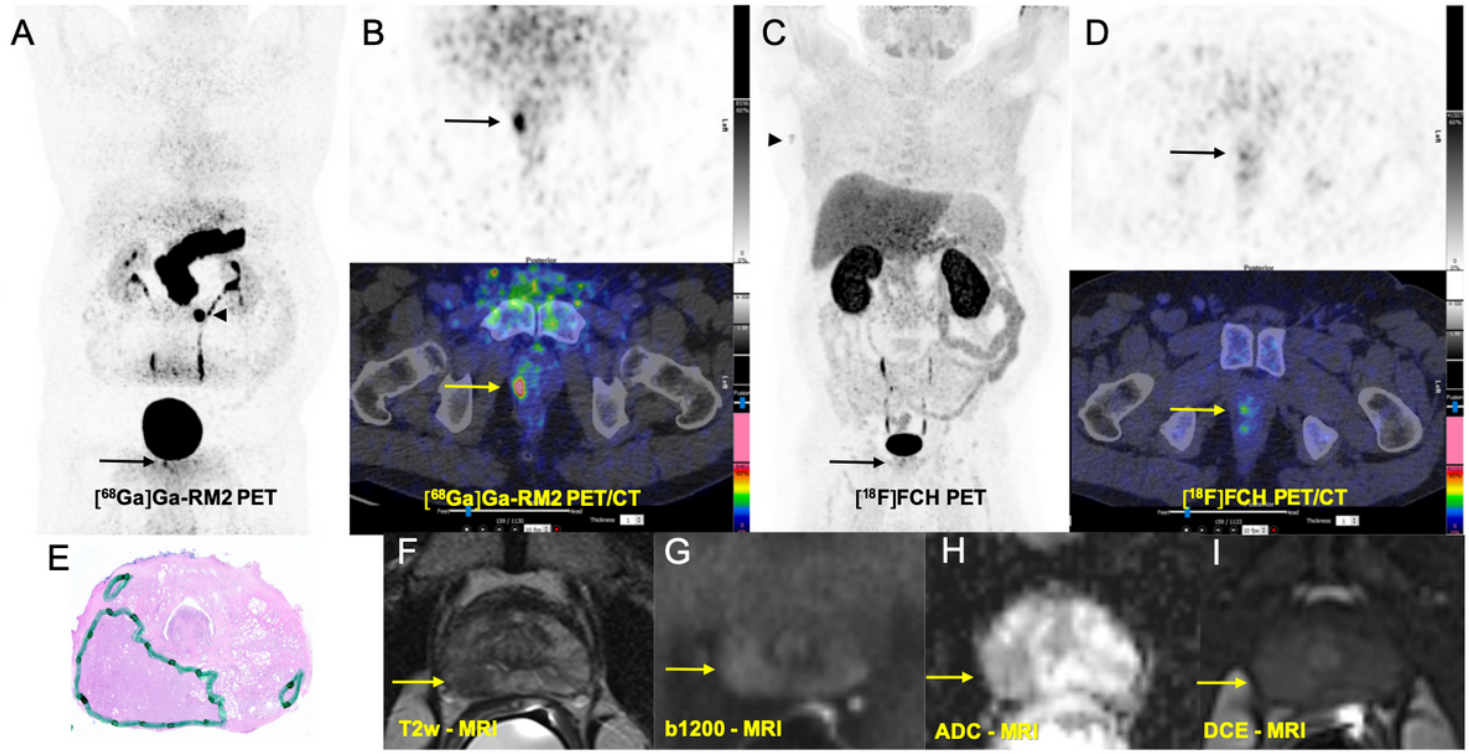

Figure 1

Comparison of [68Ga]Ga-RM2 PET/CT with [18F]FCH PET/CT and mpMRI in pre-operative staging of prostate cancer patient with intermediate risk of extraglandular metastases (PSA: 9.0 ng/ml, Gleason score: 7 (4+3), Grade 3, TNM: pT2c N0 (0/14) R0 L0 V0 Pn1) A: [68Ga]Ga-RM2 PET: Maximum Intensity Projection (MIP) shows intensive physiologic tracer uptake in the pancreas with a focal non-specific bowel uptake on the middle of left abdomen (arrow-head). A focal tracer uptake is evident in the right prostate lobe (arrow). B. Axial-view [68Ga]Ga-RM2 PET/CT (PET:upper, fusion PET/CT: middle) from prostate region showing intensive focal uptake on the left prostate lobe (arrows) corresponding with the findings on histopathology (malignany is marked) (E) [18F]FCH PET/CT MIP (C) axial-view of the prostate region (D): mild focal uptake is seen on the right axillary region, suggestive of reactive lymph node. No appreciable [18F]FCH uptake is seen on prostate. T2-weighted image (F) demonstrated a focal area of decreased signal in the left peripheral zone (yellow arrow) with corresponding diffusion weighted imaging signal restriction (trace b-values of 1200 s/mm2, G; ADC, H) and early contrast enhancement (Dinamic Contrast Enhancement, DCE, I). Overall, these findings represented a PIRADs version 2.1 score 5 lesion.

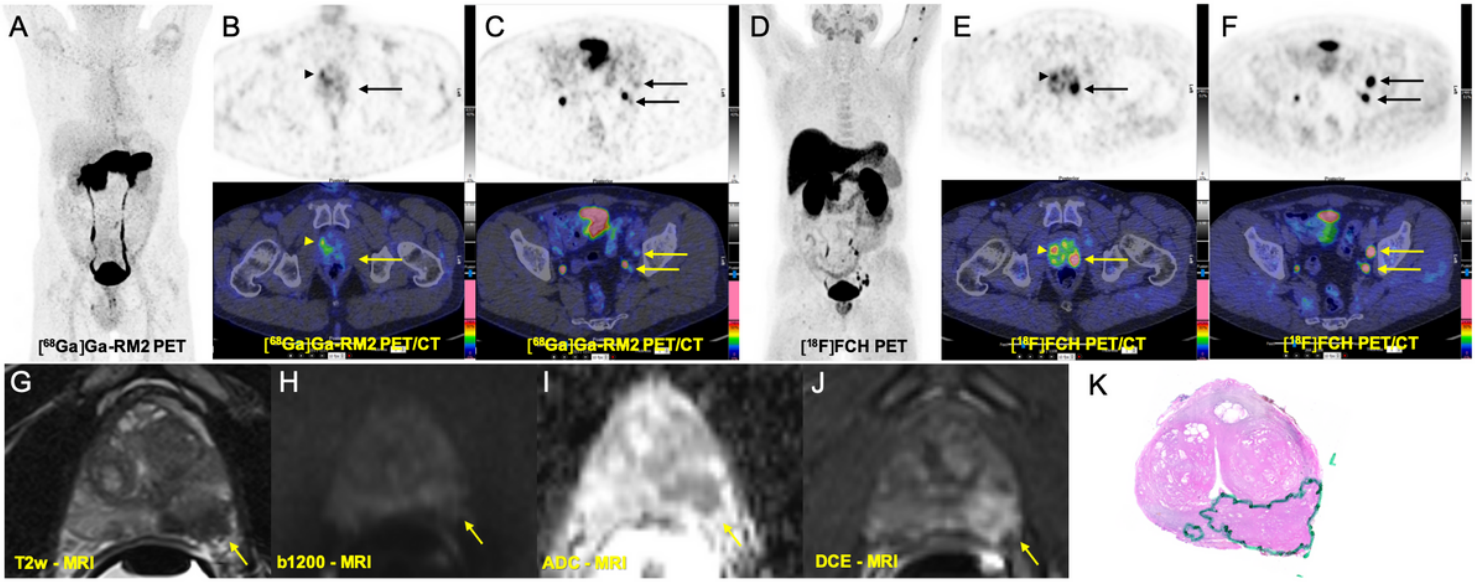

Figure 2

Comparison of [68Ga]Ga-RM2 PET/CT with [18F]FCH PET/CT and mpMRI in pre-operative staging of prostate cancer patient with high risk of extraglandular metastases (PSA: 30.0 ng/ml, Gleason score: 8 (4+4), Grade 3, TNM: pT3b pN1 (3/14) R1 (Apex li) L0 V0 Pn1) A: [68Ga]Ga-RM2 PET: Maximum Intensity Projection (MIP) shows mild focal tracer uptake on the right prostate lobe (arrow-head). B. Axial-view [68Ga]Ga-RM2 PET/CT (PET:upper, fusion PET/CT: lower row) from prostate region shows mild focal tracer uptake on the right prostate lobe (arrow-head) without corresponding malignant findings on histopathology (false positive). C: Axial-view [68Ga]Ga-RM2 PET/CT (PET:upper, fusion PET/CT: lower row) from pelvis shows only faint tracer uptakes on the lymph nodes on left iliac region (arrows). D: [18F]FCH PET/CT MIP E: Axial-view [18F]FCH PET/CT (PET:upper, fusion PET/CT: middle) from prostate region shows intensive focal tracer uptake on the left prostate lobe (arrows) corresponding with malignant findings on histopathology (K) (true positive). A focal tracer uptake is also seen on the right prostate lobe (arrow-head) without corresponding malignant findings on histopathology (false positive). F: Axial-view [18F]FCH PET/CT from pelvis shows intensive focal tracer uptakes on the lymph nodes on left iliac region (arrows), verified as metastases on histhopathology (True positive). T2-weighted image (G) demonstrated a focal area of decreased signal in the right peripheral zone (yellow arrow) with corresponding diffusion weighted imaging signal restriction (trace b-values of 1200 s/mm2, H; ADC, I) and early contrast enhancement (Dinamic Contrast Enhancement, DCE, J). Overall, these findings represented a PIRADs version 2.1 score 5 lesion.

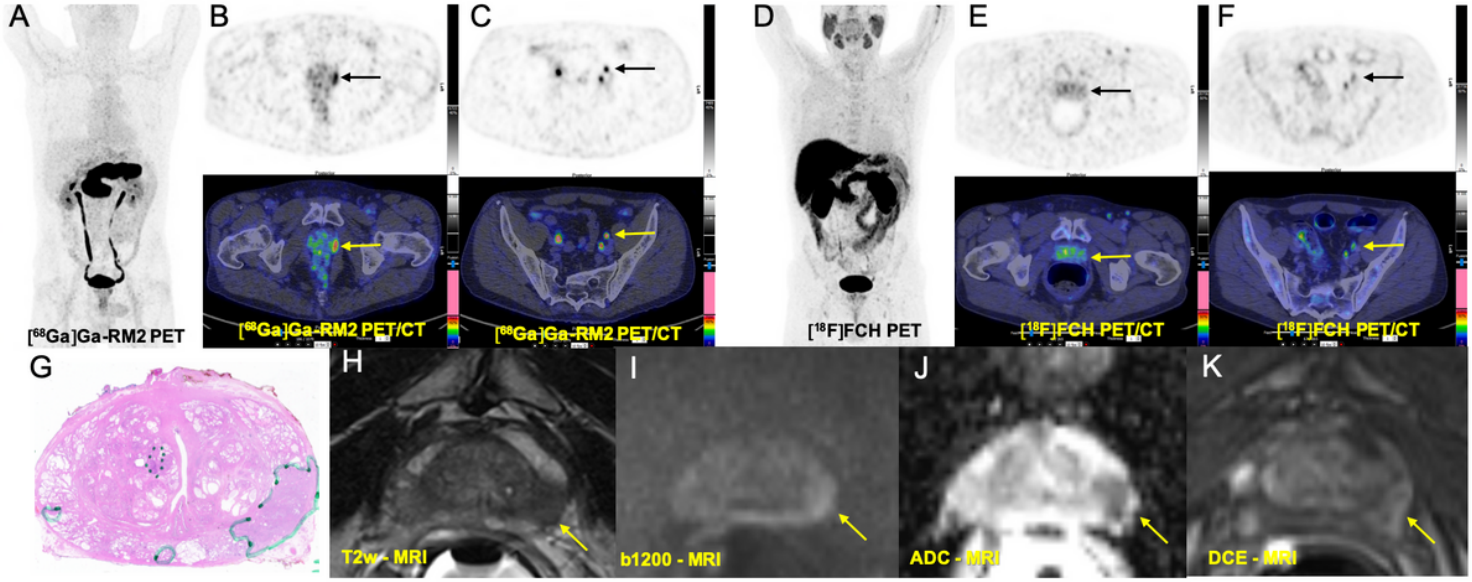

Figure 3

Comparison of [68Ga]Ga-RM2 PET/CT with [18F]FCH PET/CT and mpMRI in pre-operative staging of prostate cancer patient with high risk of extraglandular metastases (PSA: 4.49 ng/ml, Gleason score: 9 (4+5), pT3a N1 (1/23) R0 L1 V0 Pn1) A: [68Ga]Ga-RM2 PET: Maximum Intensity Projection B. Axial-view [68Ga]Ga-RM2 PET/CT ((PET:upper, fusion PET/CT: lower) from prostate region shows moderate focal tracer uptake on the left prostate lobe (arrows) corresponding to malignant finding on histopathology (G) (true positive). C: Axial-view [68Ga]Ga-RM2 PET/CT (PET:upper, fusion PET/CT: lower row) from pelvis shows focal tracer uptake on a lymph node on the left iliac region (arrows). D: [18F]FCH PET/CT MIP E: Axial-view [18F]FCH PET/CT (PET:upper, fusion PET/CT: lower row) from prostate region shows no remarkable tracer uptake on prostate (arrows) (false negative). F: Axial-view [18F]FCH PET/CT from pelvis shows only faint focal tracer uptake on the lymph node on left iliac region (arrows). T2-weighted image (H) demonstrats a focal area of decreased signal in the left peripheral zone (yellow arrow) with corresponding diffusion weighted imaging signal restriction (trace b-values of 1200 s/mm2, I; ADC, J) and early contrast enhancement (Dinamic Contrast Enhancement, DCE, K). Overall, these findings represents a PIRADs version 2.1 score 5 lesion.

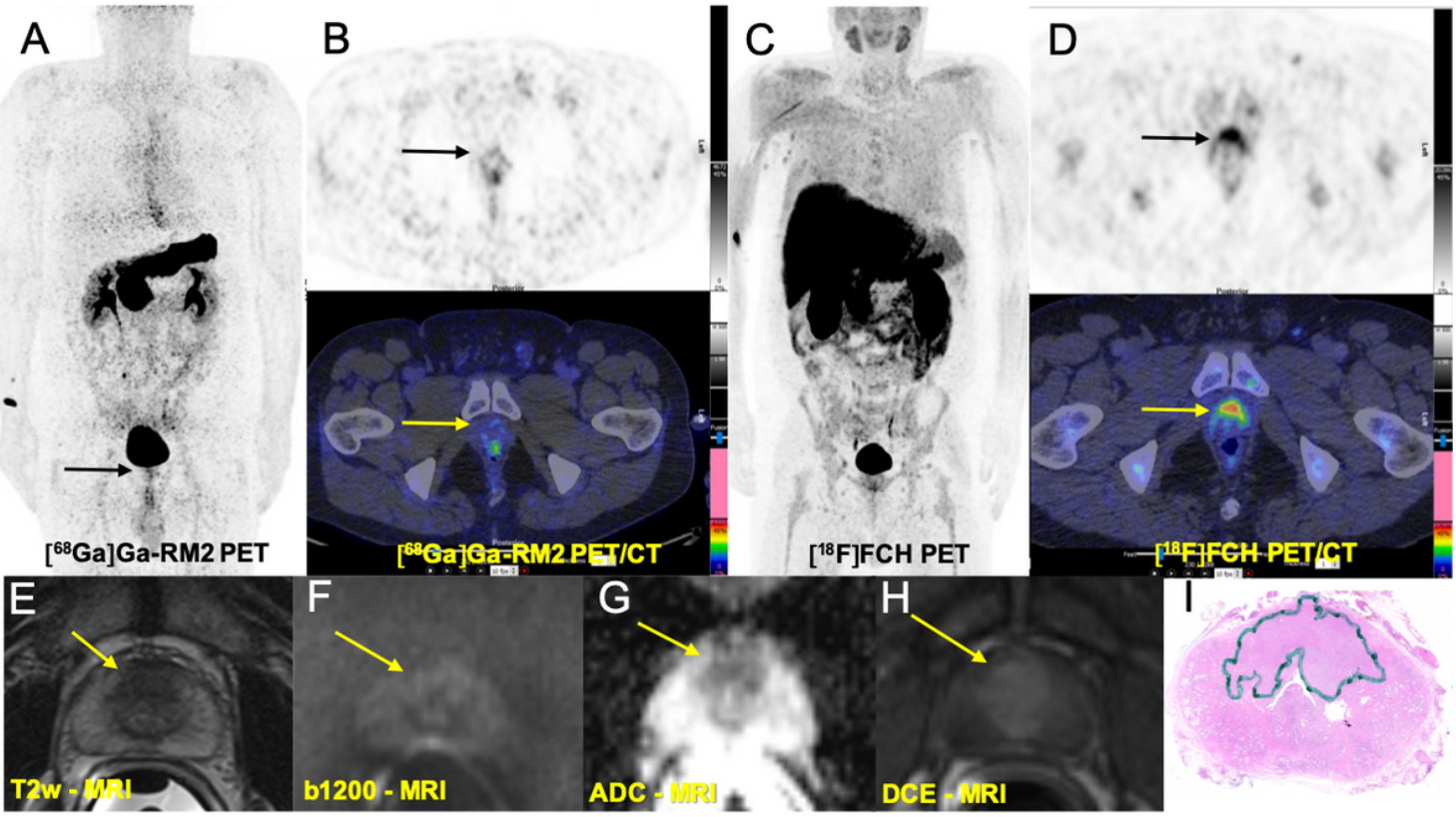

Figure 4

Comparison of [68Ga]Ga-RM2 PET/CT with [18F]FCH PET/CT and mpMRI in pre-operative staging of prostate cancer patient with high risk of extraglandular metastases (PSA: 21.6 ng/ml, Gleason score: 7 (4+3), pT3a pN0 pR1 L0 V0 pn1 A: [68Ga]Ga-RM2 PET: Maximum Intensity Projection B. Axial-view [68Ga]Ga-RM2 PET/CT (PET:upper, fusion PET/CT: lower row) from prostate region shows no remarkable tracer uptake on the (arrows) (false negative). D: [18F]FCH PET/CT MIP E: Axial-view [18F]FCH PET/CT (PET:upper, fusion PET/CT: lower row) from prostate region shows intensive tracer uptake apical anterior part of prostate (arrows) corresponding to malignant finding on histopathology (I)(true positive). T2-weighted image (E) demonstrated a focal area of decreased signal in the central gland, anterior to urethra, (yellow arrow) with corresponding diffusion weighted imaging signal restriction (trace b-values of 1200 s/mm2, F; ADC, G) and early contrast enhancement (Dinamic Contrast Enhancement, DCE, H). Overall, these findings represented a PIRADs version 2.1 score 5 lesion.

Supplementary Files

This is a list of supplementary files associated with this preprint. Click to download.

- Supplement1.docx
- Supplement2.docx